Meccanica
https://doi.org/10.1007/s11012-019-01018-y

Numerical and experimental study on mixing performance of a novel electro-osmotic micro-mixer

Azam Usefian · Morteza Bayareh

Received: 5 February 2019 / Accepted: 4 July 2019

Abstract This paper presents the numerical and experimental study on mixing enhancement in a novel electro-osmotic micro-mixer in the presence of AC and DC electric fields. PDMS is used for the fabrication of the microchip and gold nanoparticles are employed to make the electrodes. It is demonstrated that the generation of vortices due to electro-osmotic force enhances the mixing quality considerably. The strength of the vortices for DC electric field is higher than that for AC one. The results reveal that the mixing performance can be controlled by the value of applied voltage and inlet velocity of the fluids for both DC and AC electric fields. It is concluded that the mixing performance improves by enhancing the applied voltage and decreasing the inlet velocity. The experimental results are in very good agreement with the numerical ones qualitatively.

Keywords Micro-mixer · Electro-osmotic · PDMS · Vortex · Mixing efficiency

List of symbols

AC	Alternative current
C_i	Concentration at grid point i (mol/m^3)
$\overrightarrow{C_i}$	Local concentration (mol/m^3)
$\bar{C}$	Average concentration (mol/m^3)
DC	Direct current
D_i	Diffusion coefficient (m^2/s)
$\vec{E}$	Applied electric field (V/m)
E_o	(V/m)
f	Frequency (Hz)
j_i	The mass flux of the i_{th} species (kg/m^{2}s)
ME	Mixing efficiency
$\vec{n}$	Normal unit vector (m)
N	Number of nodes
p	Pressure (Pa)
t	Time (s)
$\vec{u}$	Velocity vector (m/s)
U_o	Inlet velocity (m/s)
$\vec{v}$	Liquid velocity due to electric field (m/s)
V_e	Electric potential (V)

Greek symbols

ε	Dielectric constant
ε_o	Permittivity of vacuum (C/Vm)
μ	Dynamic viscosity (kg/ms)
ρ	Density (kg/m^3)
ζ_w	Zeta potential on the inner walls (V)
σ_C	Standard deviation

1 Introduction

Micro-mixers are one of the most important components of the microfluidic devices. Rapid mixing is essential in many microfluidic applications include biochemistry analysis, drug delivery, biological

A. Usefian · M. Bayareh (✉)
Department of Mechanical Engineering, Shahrekord University, Shahrekord, Iran
e-mail: m.bayareh@sku.ac.ir

Published online: 12 July 2019

processes etc. [1–3]. Micro-mixers are divided into active and passive ones. Passive micro-mixers use special geometry [4–8] and flow characteristics [9, 10] to improve the mixing performance. Active micro-mixers require an external force to increase mixing quality. Electro-kinetic approaches such as electro-osmotic and electrophoresis techniques as active micro-mixers employ alternative current (AC) or direct current (DC) electric fields to enhance the mixing efficiency. Most of the investigators have studied the enhancement of the mixing efficiency in the electro-osmotic micro-mixers numerically. For example, Chen et al. [11] studied the mixing of fluids in an active electro-osmotic micro-mixer. Their micro-mixer is a reference for evaluating the influence of electric field on mixing performance of micro-mixers. Their micro-mixer included two inlet and outlet micro-channels and a central loop between them. Four micro-electrodes were placed on the outer wall of the circular loop symmetrically. They neglected the transient effects by assuming that the electric field is quasi-steady. They demonstrated that the fluid particles are affected by the electric field and exhibit stretching and folding in the central loop indicating chaotic advection and molecular diffusion during the mixing process. Seo et al. [12] compared the mixing quality of a ring-type electro-osmotic micro-mixer with circular and rectangular obstacles. They confirmed that the stretching and folding occur for two configurations, however circular obstacle exhibits a smoother pattern and higher mixing efficiency than the rectangular one. Zhou et al. [13] introduced an optimized electro-osmotic micro-mixer in comparison with the reference one. They demonstrated that their micro-mixer with asymmetrical structure increases the fluctuations in the flow leads to an enhancement of folding and stretching of the flow. Shamloo et al. [14] revealed that the mixing quality decreases as the inlet velocity of fluids increases. It was concluded that electro-osmotic force has larger effect than inertial force. They simulated the mixing process in a two-ring configuration micro-mixer and found that the mixing efficiency enhances by 99%. Shamloo et al. [15] improved the geometry of the reference micro-mixer and introduced a T-shaped micro-mixer equipped with a chamber in the middle. They studied the effect of different parameters on the mixing performance in the presence of DC power supply.

Mixing quality was evaluated using different distribution of micro-electrodes in various types of micro-channel wall by Meng et al. [16]. They showed that the vortex generated in the vicinity of the interface of the fluids has a crucial effect on mixing process. They employed DC and AC electric fields and demonstrated that the stability of the micro-mixer for DC electric field is higher than that for AC one. Cheng et al. [17] exerted AC voltages to a T-shaped micro-mixer using four electrodes. They revealed that the frequency of 200 Hz is an optimum magnitude leads to the maximum efficiency. Shamloo et al. [14] also showed that there is an optimal frequency of voltages for one ring electro-osmotic micro-mixer. Recently, Usefian et al. [18, 19] demonstrated that the mixing quality enhances with the frequency and voltage. They revealed that the angular velocity of inner obstacle can improve the mixing efficiency significantly. The authors reported that the mixing efficiency is about 98% for the angular velocity of 1.148 rad/s. It was also found that the mixing quality increases with applied electric current in the presence of magnetic field for Newtonian and non-Newtonian liquids. In addition, Chen and Wu [20] showed that as the frequency increases, the mixing effect increases for a micro-mixer with three pair electrodes. They also confirmed that the mixing efficiency is an increasing function of voltage.

To the best of our knowledge, there is a few experimental investigations considering the influence of electric field on mixing performance of micro-mixers. Sasaki et al. [21] discussed different experimental conditions to evaluate the mixing characteristics of an AC electro-osmotic micro-mixer. Two micro-electrodes having a sinusoidal gap were placed on the bottom of the channel. However, they did not present the time evolution of recorded images.

In the present study, a novel electro-osmotic micro-mixer equipped with a pair of electrodes is introduced (Fig. 1). The micro-electrodes having an optimal distance are placed on the bottom of the chamber. The mixing enhancement of the micro-mixer is investigated numerically and experimentally by applying AC and DC electric fields. Since the installation of electrodes in the micro-channel wall has been a great challenge, the main objective of the present study is to evaluate the mixing quality in practical applications in comparison with the numerical simulations. The numerical simulations are

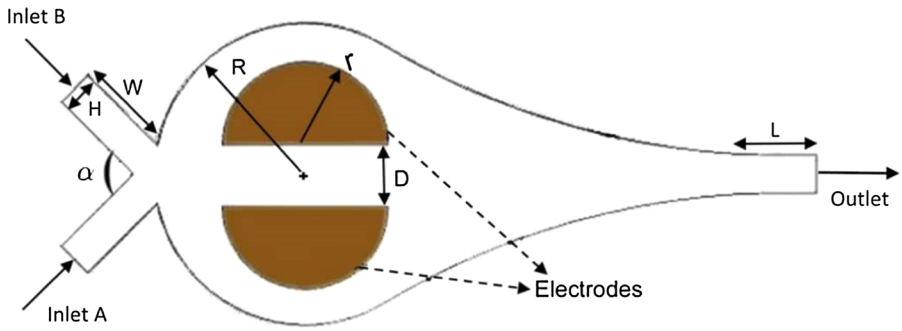

Fig. 1 Schematic of the proposed micro-mixer (top view): H = 200 μm, W = 900 μm, L = 500 μm, R = 1000 μm, r = 250 μm, D = 300 μm, and α = 90°

performed using Comsol Multiphysics 5.3 software. The paper is organized as follows: the experiments are described in Sect. 2. In Sect. 3, the governing equations and numerical method are presented and the results are discussed in Sect. 4. Conclusions are presented in Sect. 5.

2 Experimental setup

The mold of the microfluidic mixer is fabricated by soft lithography technique. Polydimethylsiloxane (PDMS) is employed to fabricate the microchip. PDMS is a flexible and transparent elastomer that is widely used in microfluidics. In its structure, two methyl groups are attached to silicon atoms. It is insoluble in water and has the density of 0.971 kg/m^3. The micro-mixer consists of a circular micro-chamber of 1000 μm connected to a nozzle-shaped channel. Two straight channels with 250 μm in width, 250 μm in depth and 900 μm in length provide the inlet channels that deliver two liquid streams into the micro-mixer. A pair of electrodes are placed on the bottom of the circular chamber. The electrical voltage is applied to the electrodes that have positive and negative voltages. Gold nanoparticles are used to make electrodes. Due to the sensitivity of the experiments and no reaction of the electrodes with the solution, the best choice is the gold metal. To make electrodes, a 100 nm thin layer of gold is deposited on a glass (lam) (Fig. 2).

Pure water with a blue pigment color and potassium chloride 20 mM with a red pigment color are injected by a syringe pump from inlets A and B, respectively. A very small amount of food colors is used to visualize the flow field. The volumetric flow rate of 0.1 ml/min (U_o = 0.23 mm/s) is applied in each inlet and the flow rate of the inlets is identical. The range of applied voltages is 5 V to 30 V and the frequency for AC electric field is 0.5 Hz. The temperature of laboratory is kept at 20 °C that is used to determine its properties for relevant simulations. The mixing process is recorded by a 1000× digital microscope. A picture of the experimental system is shown in Fig. 3.

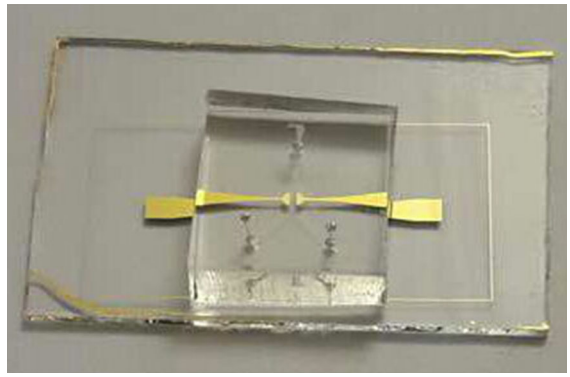

Fig. 2 Fabricated micro-mixer with a pair of golden electrodes

3 Governing equations

Utilization of AC or DC electric fields induces electro-osmotic flow. The interaction between two phenomena is the origin of the electro-osmotic flow when AC or DC voltages are applied. These phenomena are the tangential electric field and charged liquids at electrical double layer on the electrodes [21]. Therefore, the liquids flow from the middle of the electrode gap to the opposite side of the electrodes. For the case of DC

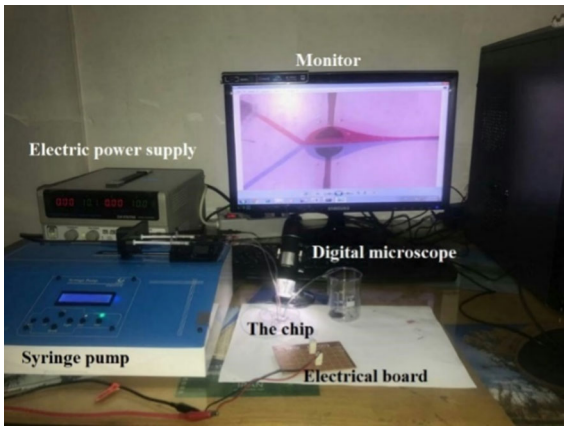

Fig. 3 A picture of the experimental system

electric field, the flow direction changes periodically depends on the voltage and frequency.

The governing equations for a Newtonian incompressible flow are continuity and Navier–Stokes equations:

$$\nabla \cdot \vec{u} = 0 \tag{1}$$

$$\rho\left(\frac{\partial \vec{u}}{\partial t} + \vec{u}.\nabla\vec{u}\right) = -\nabla p + \mu\nabla^2\vec{u} + \rho_e\vec{E} \tag{2}$$

where $\vec{u}$ indicates the velocity vector, p is the pressure, ρ is the density and μ is the dynamic viscosity. There is no pressure gradient in whole flow field. Fully developed laminar flow is imposed on the inlet of the channel and no normal stress boundary condition is used for the outlet of the channel. In the present simulations, electro-osmotic slip velocity is used for all walls. Hence, the term $\rho_e\vec{E}$ is ignored in the momentum equation. By applying this boundary condition, electro-osmotic flow is generated. It displaces the charged liquids in the electrical double layer. This thin layer is modeled by Helmholtz–Smoluchowski relation. Based on this relation, the electric field imposes a force on the liquid close to the electrodes. Hence, the liquid moves in the direction of the electric field with the following velocity [14]:

$$\vec{v} = -\frac{\varepsilon_o\varepsilon\zeta_w}{\mu}\vec{E} \tag{3}$$

where ζ_w denotes zeta potential on the inner walls which is equal to -0.1 V, $\vec{E}$ indicates the applied electric field, ε is dielectric constant which is equal to 80.2, and ε_o refers to permittivity of vacuum that is equal to 8.854×10^{-12} C/Vm.

In addition, the initial condition of the flow velocity is set as zero, e.g. $\vec{u}|_{t=0} = 0$. In other words, the simulations are performed by considering stationary solution at t = 0 s. The solutions of stationary simulations are used for time-dependent simulations. It should be mentioned that the term of electric field is coupled with the momentum equation only for time-dependent simulations [14].

The electric potential V_e is applied in the liquid and is calculated by the following Laplace equation:

$$\nabla^2 V_e = 0 \tag{4}$$

where $\vec{E} = -\nabla V_e$. Boundary condition is imposed on the electrodes are presented in Eqs. 5 and 6 for AC and DC electric fields, respectively:

$$V = V_o Sin(2\pi ft + E_o) \tag{5}$$

$$V = V_o \tag{6}$$

where V_o is the maximum AC potential. All boundaries except the electrodes are electrical insulated.The convection–diffusion equation is used for the mixing fluid [14]:

$$\nabla \cdot \overrightarrow{j_i} = 0 \tag{7}$$

where j_i is the mass flux of the i_{th} species that is defined as:

$$\overrightarrow{j_i} = -D_i\nabla\overrightarrow{C_i} + \vec{u}\overrightarrow{C_i} \tag{8}$$

where $\overrightarrow{C_i}$ is the local concentration and D_i indicates the diffusion coefficient that is 10^{-11}m^2/s.

The boundary conditions for the concentration field are as follows: $C = 20$ mM for stream A (potassium chloride), and $C = 0$ for stream B (pure water). In addition, no flux boundary is imposed on the other boundaries:

$$\vec{n} \cdot \left(-D_i\nabla\overrightarrow{C_i} + \vec{u}\overrightarrow{C_i}\right) = 0 \tag{9}$$

All governing equations are solved using finite element approach. In addition, Generalized Minimum Residual Method (GMRES) is employed by Comsol Multiphysics 5.3 software.

Mixing efficiency, ME, is calculated to quantify the performance of the micro-mixer:

$$ME = 1 - \frac{\left[\sum_{i=1}^{N} \frac{(C_i - \bar{C})^2}{N}\right]^{1/2}}{\bar{C}} \approx 1 - \frac{\sigma_C}{\bar{C}} \qquad (10)$$

where σ_C and $\bar{C} = \sum_{i=1}^{N} C_i/N$ are the standard deviation and the average concentration, respectively. N denotes the number of nodes in the considered area. Therefore, ME = 100% indicates a perfect mixing. In the present simulations, N = 20 and the cross-sectional area is located at the output of the micro-channel.

4 Results

The electrodes were placed on the channel walls of micro-mixers in previous numerical studies. It is practically so difficult to put the electrodes on the channel walls. Due to the limitations in the manufacture of micro-mixers, a novel micro-mixer is proposed to ease the fabrication and layering of electrodes to conduct the experiments. This micro-mixer, in addition to its simplicity, has a relatively large chamber contains a large volume of fluid and the mixing is carried out during a very short period of time.

4.1 Verification of the numerical scheme and grid study

Since the present study include numerical simulations, the results of the present work are compared with the present experimental results and the numerical results of Shamloo et al. [14], which obtained the mixing efficiency for a two-ring micro-mixer (Figs. 2, 3 and 4a). Shamloo et al. [14] applied the AC electric field using four electrodes for each ring and determined the mixing efficiency based on optimized variables. Figure 4b shows the mixing efficiency at different times for the outlet of the micro-mixer. This figure shows that the efficiency of the fluid mixing is more than 99%, which is predictable due to the presence of the second ring. This figure represents that the present results are in excellent agreement with the results of Shamloo et al. [14].

The numerical simulations should be independent of the number of grid points. Therefore, the mixing efficiency is calculated for four grid resolutions. Figure 5 shows that the results are independent of mesh size for further mesh refinement than 11,182 grid points. Because the computing time is proportional to the grid size, the grid resolution of 11,182 is selected for further simulations. In addition, similar simulations are performed for the case of DC electric field when f = 0.5 Hz and it is demonstrated that the grid resolution of 11,182 is sufficient for the simulations. Figure 6 shows the mesh distribution in the computational domain. The characteristics of the grid are as follows: maximum and minimum element sizes for entire geometry are 1.5 μm and 0.0055 μm, respectively. These values for electrode boundaries are 1.9 μm and 0.021 μm, respectively.

4.2 The optimal distance between two electrodes

To design and fabricate the proposed microfluidic chip, the optimal electrode gap in the mixing chamber should be determined. Figure 7 shows the mixing efficiency along the micro-mixer for different distances between the electrodes. The results demonstrate that the optimal distance is about 300 μm. Hence, less

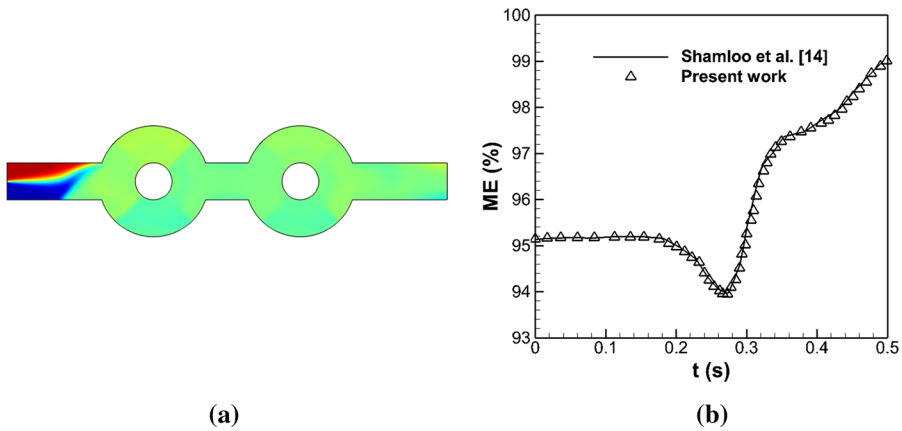

Fig. 4 Comparison between the present results and the ones of Shamloo et al. [14]: **a** distribution of fluid concentrations for the micro-mixer at 0.5 s, and **b** the mixing efficiency versus time for $U_o = 0.05$ mm/s, $V_o = 0.5$ V and f = 4 Hz

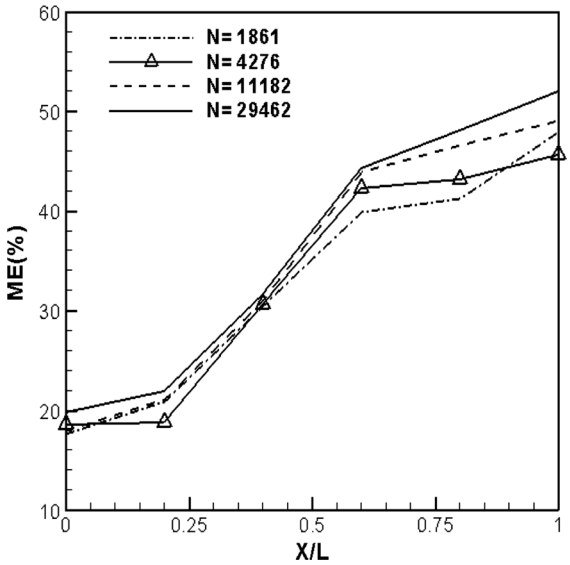

Fig. 5 The mixing efficiency along the micro-mixer for different grid resolutions under AC electric field, $U_o = 0.23$ mm/s and $V_o = 15$ V

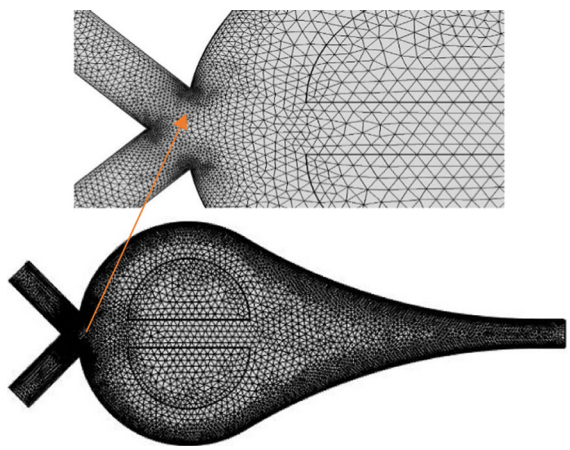

Fig. 6 The mesh distribution in the computational domain

liquids are affected by the applied voltage for the distance less and more than 300 μm. A reduction in the electric field leads to a reduction in the strength and number of vortices in the circular chamber. Therefore, the mixing performance decreases. For example, the mixing efficiency for the electrodes at the distance of 250, 300, and 400 μm is about 46%, 52%, and 48%, respectively.

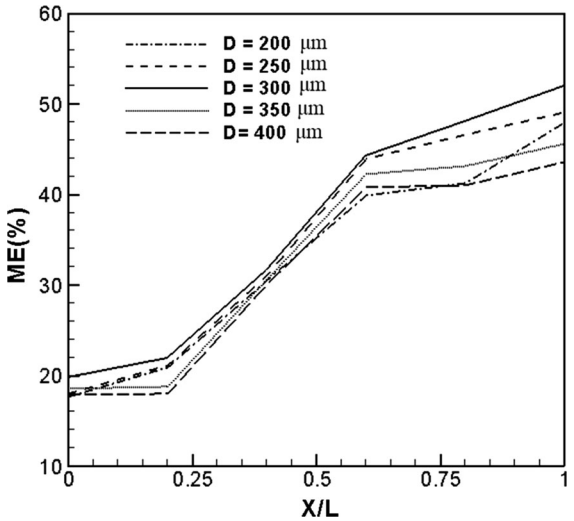

Fig. 7 Mixing efficiency along the micro-mixer for different distances between electrodes under AC electric field, $U_o = 0.23$ mm/s and $V_o = 15$ V

4.3 Effect of AC and DC electric fields

To evaluate the mixing efficiency under AC and DC electric fields, these two fields are applied to the electrodes with the optimum distance of 300 μm numerically and experimentally. Figure 8 shows concentration and streamlines profiles for different electric fields. The figure reveals that as the voltage increases, the mixing quality increases. In the absence of an electric field, the mixing depends on molecular diffusion. The vortices are not formed when the electric field is not applied. However, the flow field is affected by the electric fields in the vicinity of the electrodes and the liquids rotate in these regions. Different signs of zeta potential result in the induction of electro-osmotic flow that causes the flow to rotate. In the electrical double layer, there is a negative net charge that produces a negative flow towards the micro-mixer inlet in the areas with positive zeta potential, and vice versa, the flow direction is toward the micro-mixer outlet in the regions with a negative zeta potential. Therefore, in order to satisfy the continuity condition of flow, a fluid rotation occurs and subsequent vortices are created. Vortices are formed around the electrodes and gradually fill the entire chamber. The figure indicate that the application of DC electric field is more suitable and causes higher stretching and folding of the fluid layers. In other

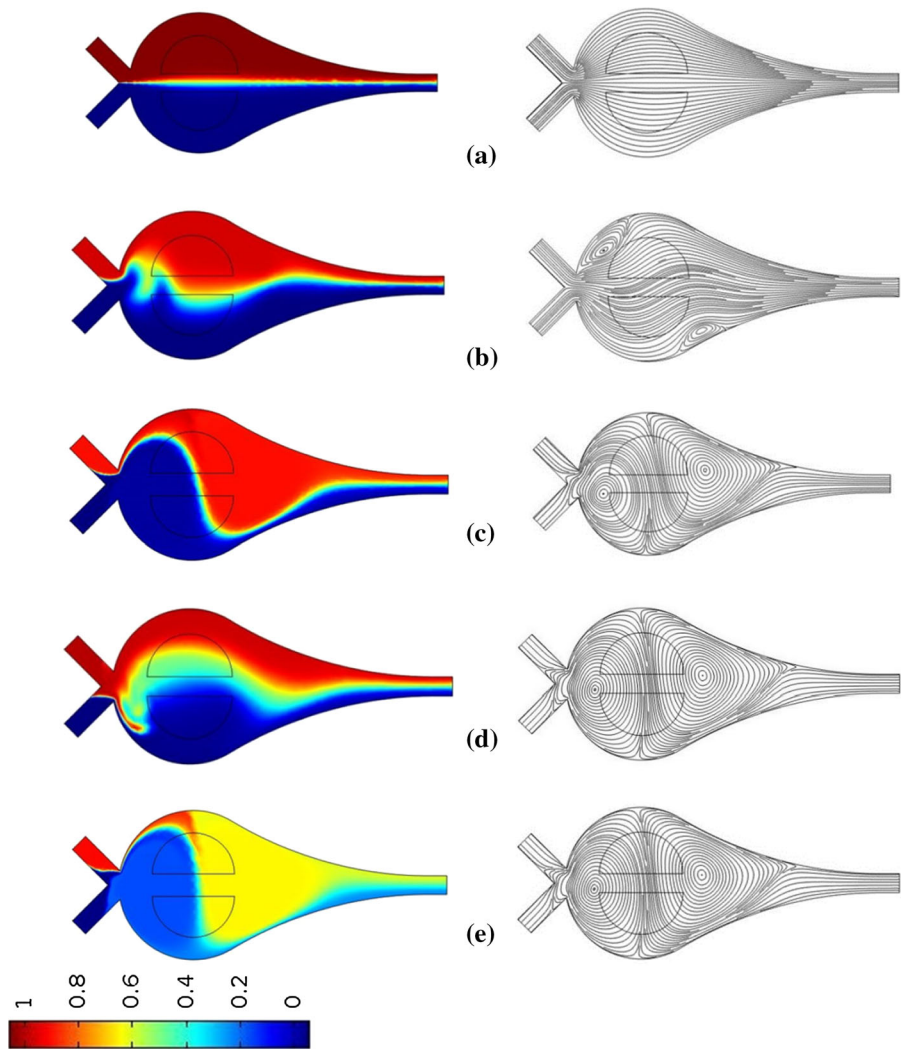

Fig. 8 Streamlines (right) and concentration profiles (left) for $U_o = 0.23$ mm/s: **a** without applying the electric field, **b** AC electric field: f = 0.5 Hz and $V_o = 15$ V, **c** DC electric field: $V_o = 15$ V, **d** AC electric field: f = 0.5 Hz and $V_o = 30$ V, and **e** DC electric field: $V_o = 30$ V

words, the application of a direct electric field leads to a higher mixing in the outlet.

Concentration and streamlines profiles show that vortices are formed throughout the mixing chamber by applying a direct electric field. The vortex strength increases with increasing the voltage. By applying the electric field, the formation of electrical layer results in the displacement of the material layers of two fluids and displaces their boundary. In the direct electric field, this displacement starts from the micro-channel inlet and continues to the channel convergence section. Expansion vortices are generated at the convergence area. These vortices cause a great disturbance at low Reynolds numbers leads to an enhancement in the mixing efficiency. When the alternating electric field is applied, the vortices are formed in the vicinity of the electrodes and only affect the fluid flow in this region. The alternating current is an electric current of which value and direction vary with the time. Since the current magnitude and the direction of motion of the electrons vary (from the maximum to zero and from zero to minimum), causing a distortion and turbulence in the vicinity of the electrodes. The vortices are created on the sides of the walls and do not occupy the middle part of the chamber. In other words, the effect of the central vortices is lost, leading to a reduction in the flow rotation. The vortices that are created due to AC electric field are smaller and weaker than the vortices generated due to DC electric field. Therefore, according to the proposed geometry, AC electric field is not

appropriate for the mixing of liquids in comparison with DC one.

As shown in Fig. 9, the mixing efficiency increases dramatically in the presence of DC electric field. The mixing efficiency is about 21% in the mixer outlet in the absence of electric field. It increases by 40.14% due to the application of an AC electric field with a frequency of 0.5 Hz and a voltage of 15 V after 2 s. But after applying a DC electric field with a voltage of 15 V, the mixing efficiency is about 51.18% after 0.1 s. The concentration profile obtained from the numerical simulations also indicate the superiority of the DC electric field. The fluid layers have a high stretching and folding due to the formation of the electric sub-layer. The mixing efficiency at the outlet of the micro-mixer reaches 81.16% by applying the DC electric field. By applying an AC electric field at the voltage of 30 V, the mixing efficiency increases by 43.39%. It can be concluded that the application of an electric field results in the change in the direction of the fluid due to the zeta potential close to the walls. Hence, the direction of flow varies and contact surface of the two fluids increases leads to an enhancement in the molecular diffusion.

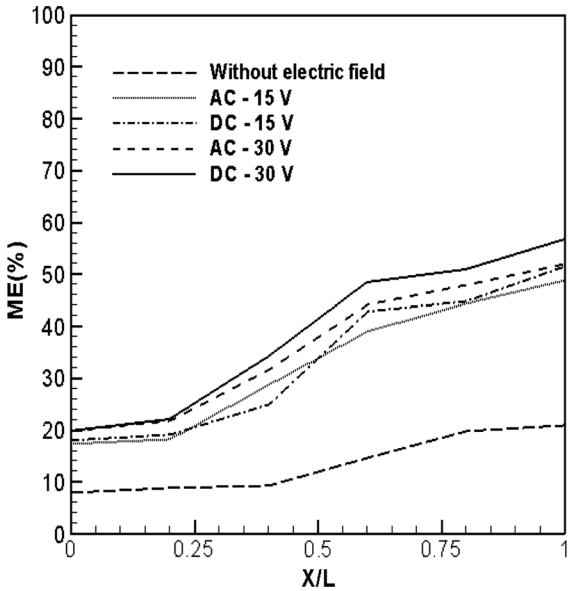

Fig. 9 The effect of DC and AC electric fields on the mixing efficiency along the micro-mixer at $U_o = 0.23$ mm/s and $V_o = 15$ V

Comparison of the present numerical and experimental results is shown in Fig. 10. This figure confirms that AC and DC electric fields improve the mixing performance of the proposed micro-mixer. Experimental results also confirm that the stretching and folding of material lines of fluids is affected by the

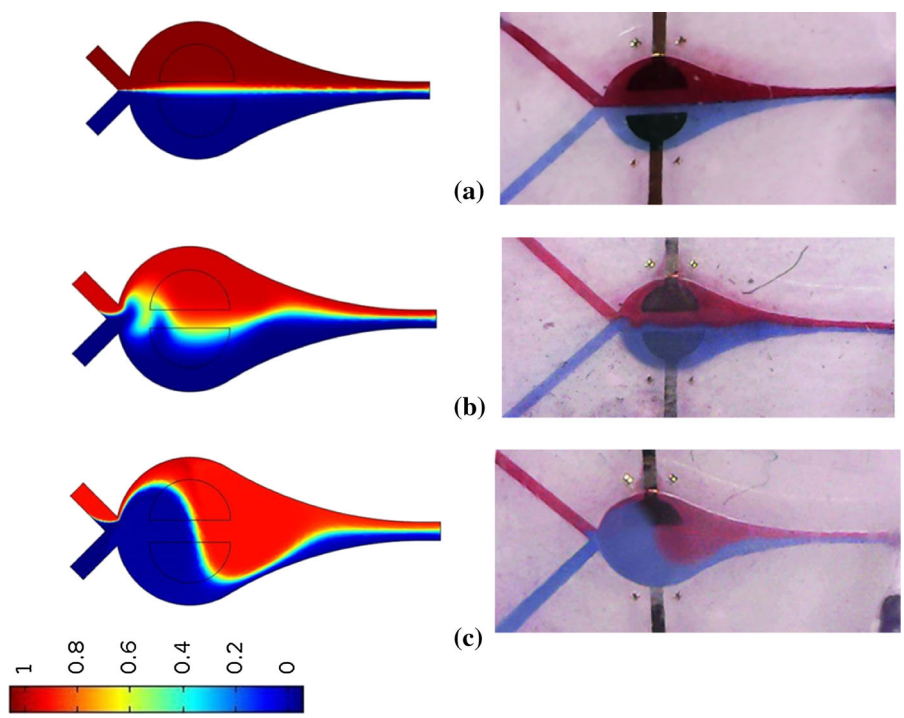

Fig. 10 Distribution of fluid concentrations; experimental results (right) and results obtained from the numerical simulation (left) at $U_o = 0.23$ mm/s: **a** without applying the electric field, **b** AC electric field: f = 0.5 Hz and $V_o = 15$ V, and **c** DC electric field with $V_o = 15$ V

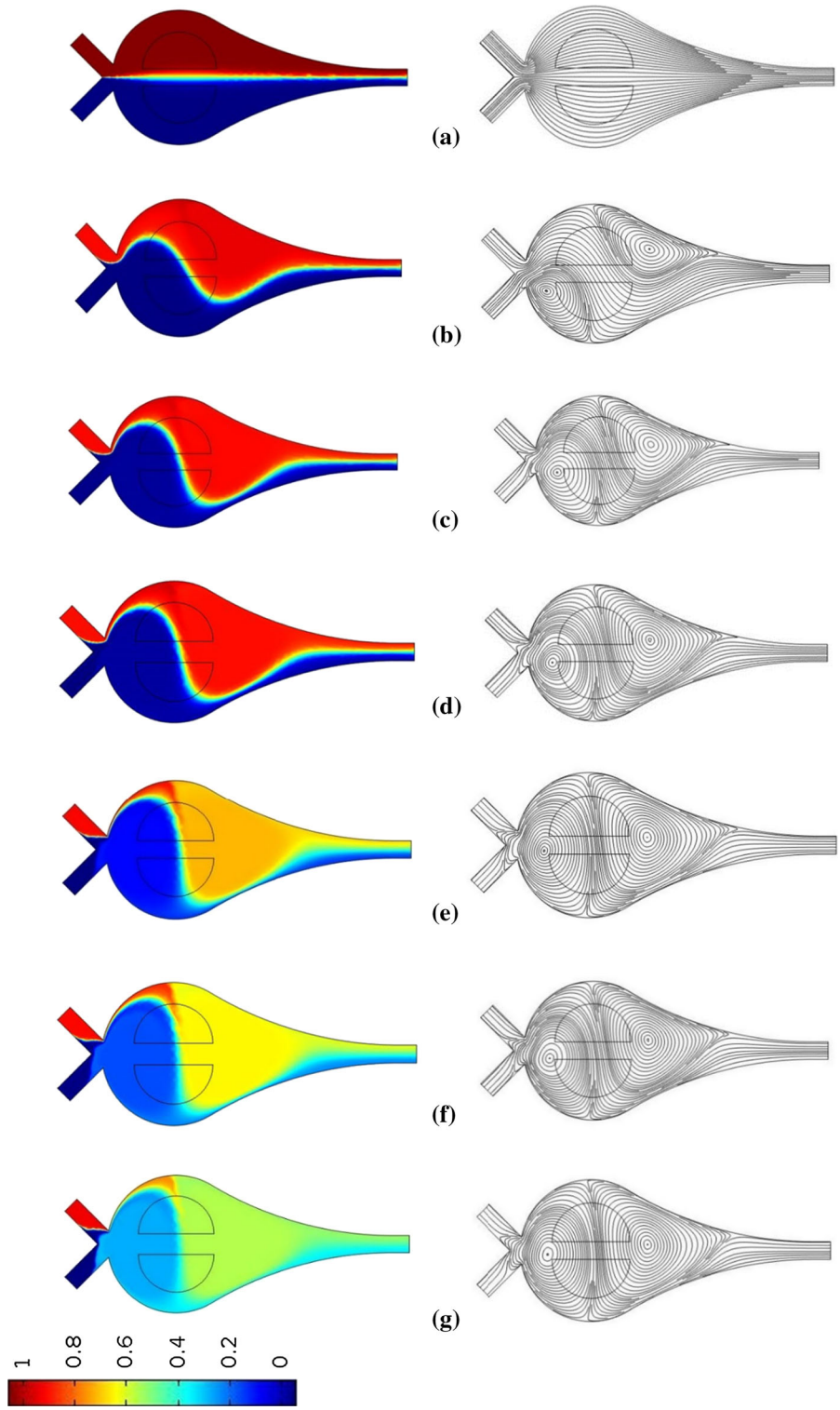

Fig. 11 Streamlines (right) and concentration contours (left) in the presence of DC electric field for $U_o = 0.23$ mm/s: **a** $V_o = 0$ V, **b** $V_o = 5$ V, **c** $V_o = 10$ V, **d** $V_o = 15$ V, **e** $V_o = 20$ V, **f** $V_o = 30$ V and **g** $V_o = 40$ V

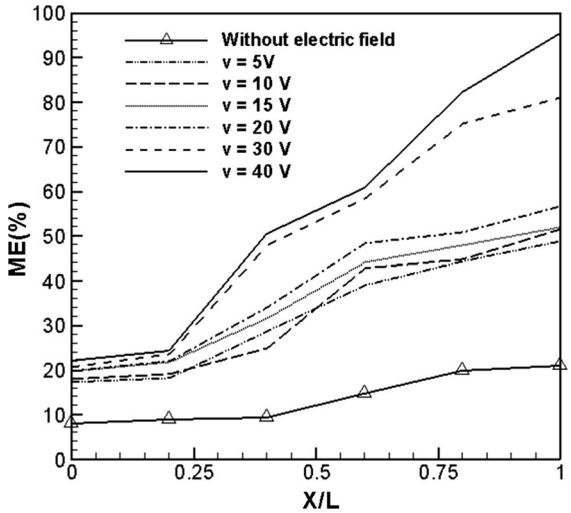

Fig. 12 Mixing efficiency along the micro-mixers for DC electric field and different voltages for $U_o = 0.23$ mm/s

electric field. For the case of AC electric field, the displacement of fluid layers is approximately limited to the interface for the voltage of 15 V. However, the size of vortices for DC electric field is much larger than that for AC one. It is also worth noting that there is a very good agreement between the simulation and experimental results.

4.4 Effect of the voltage

To investigate the effect of the voltage on mixing efficiency, the voltage range of 5–40 V is applied by DC electric field. Figure 11 shows the concentration contours and streamlines obtained from numerical simulations for different voltages. The vortices are formed due to the slip velocity of the fluids in the vicinity of the walls caused by the application of the zeta potential. The slip velocity increases with the voltage results in the formation of more vortices in the chamber. These vortices cause disturbances along the flow at low Reynolds numbers. They affect the fluid material layers and improve the mixing by creating irregular displacements. In the vicinity of the electrodes and in the space between the walls of the microchannel leading to the outlet side, expansion vortices are generated. These vortices create the electroosmotic velocity, which causes irregular displacement and high molecular diffusion leads to high mixing index [14, 22].

Figure 12 shows the mixing efficiency along the micro-mixer for different DC voltages. This figure demonstrates that the mixing efficiency varies from 21% (for $V_o = 0$ V) to 95.56% (for $V_o = 40$ V), which means that the mixing is almost completed. The

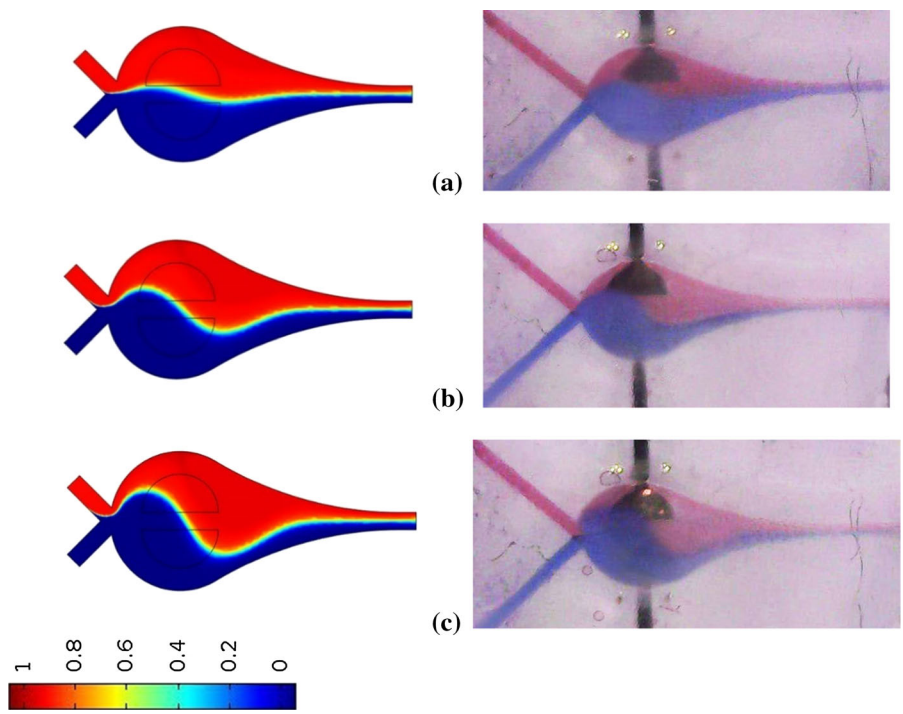

Fig. 13 Fluid concentration profile in a micro-mixer; experimental results (right) and results obtained from numerical simulations (left) for $U_o = 0.23$ mm/s and DC electric field with $V_o = 5$ V at the time: **a** 0.0525 s, **b** 0.961 s and **c** 0.1 s

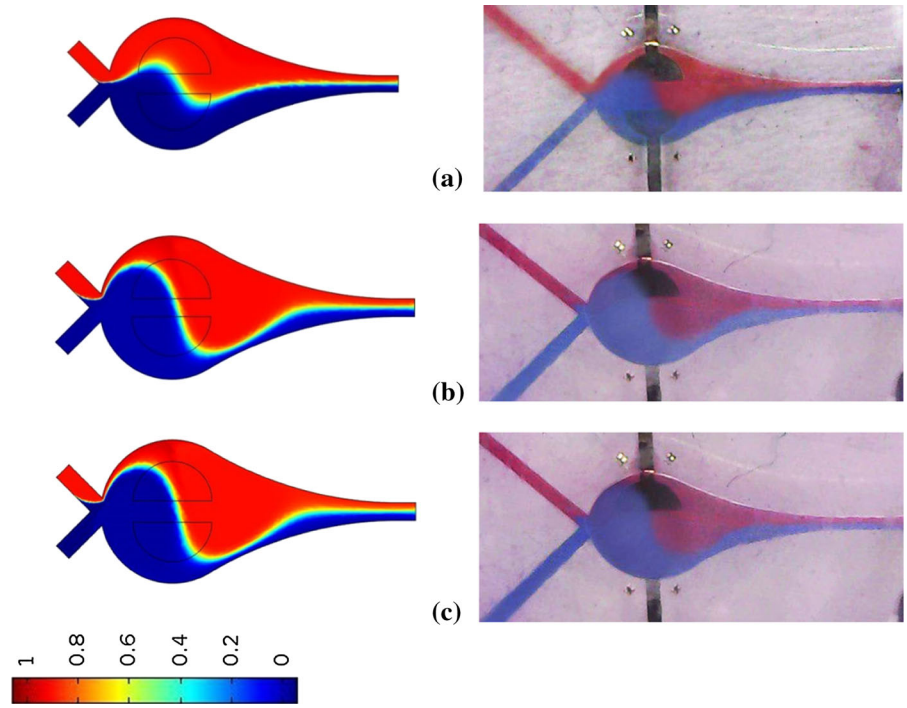

Fig. 14 Fluid concentration profile in a micro-mixer; experimental results (right) and results obtained from numerical simulations (left) for $U_o = 0.23$ mm/s and DC electric field with $V_o = 15$ V at the time: **a** 0.0345 s, **b** 0.095 s and **c** 0.1 s

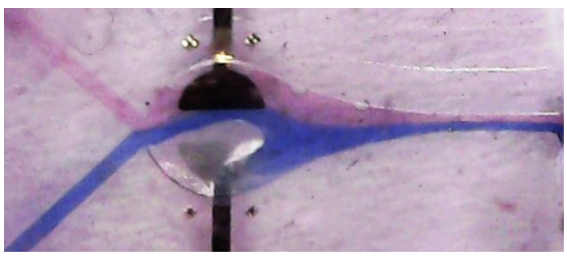

Fig. 15 Bubbles generated in the liquid flow under DC electric field with $V_o = 30$ V

mixing efficiency increases from 21 to 47% for the voltages 0–5 V. In the range of 10–20 V, the mixing efficiency enhances about 4%, however the voltage value has a significant effect on the mixing efficiency for the range of 20–40 V. The mixing efficiency of 56.87% at 20 V reaches 81.61% and 95.56% at 30 and 40 V, respectively. It can be concluded that the rate of enhancement of mixing quality is higher for greater voltages.

The electrodes act like a capacitor by applying the electric field and affect a large volume of fluid. As the voltage increases, the fluid layers are highly disturbed due to the heat generated by the electricity. The electric field strength increases with the voltage and therefore the slip velocity resulting from the Zeta potential within the chamber produces micro-vortices [22]. These vortices improve the mixing quality significantly.

Figures 13 and 14 present the comparison of the concentration profile according to present numerical and experimental results for the voltages of 5 and 15 V in the presence of DC electric field. The mixing process takes place in 0.1 s, which is an extremely fast and desirable time for most biological processes, sensitive chemical and enzymatic reactions. The figures exhibit very good agreement between the present numerical and experimental results.

Although the mixing efficiency increases proportional to the voltage due to the vortex strengthening, bubbles may be generated at high voltages and the mixing process is in trouble. The present experimental results demonstrate that when the voltage as high as 25 V, bubbles appear in the chamber. Bubbles are generated for a variety of reasons. One of the reasons is that higher voltages produce heat inside the chamber and liquid particles evaporate and appear in the bubble form. Another reason is the melting of gold nanoparticles from the surface of the electrodes. The electrodes operate with a specific voltage, such as a capacitor, according to the conditions of fabrication and layering. At higher voltages, it will lose its

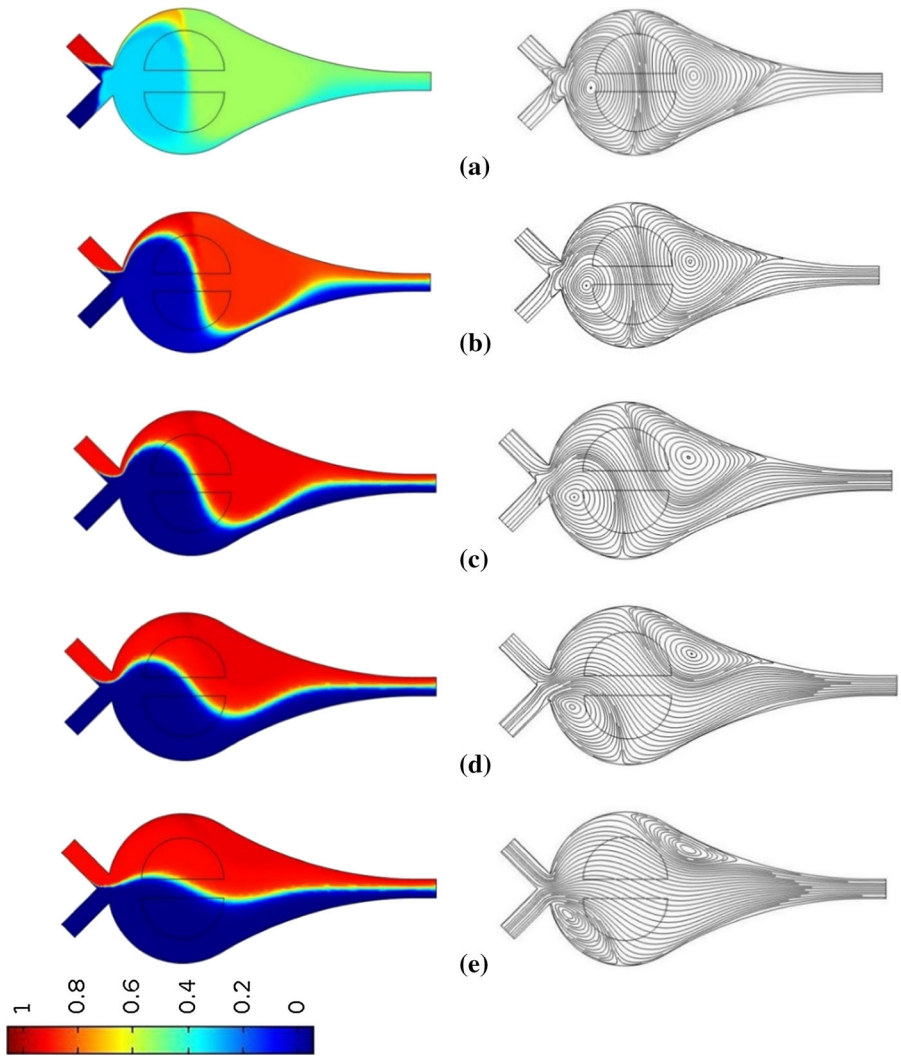

Fig. 16 Streamlines (right) and concentration contours (left) in the presence of DC electric field with $V_o =$ 15 V and: **a** $U_o = 0.115$ mm/s, **b** $U_o = 0.23$ mm/s, **c** $U_o = 0.46$ mm/s, **d** $U_o = 0.92$ mm/s, **e** $U_o = 2.3$ mm/s

strength due to overheating and may even react with fluid particles. As shown in Fig. 15, the bubbles appear close to the electrode connected to the positive voltage of power supply. The occurrence of bubbles was also observed by Shang et al. [23] who investigated the mixing enhancement in a micro-mixer using a piezoelectric disk attached to the mixer.

DC electric field is more effective to enhance the mixing efficiency for the proposed micro-mixer considering the position and number of electrodes. However, the enhancement in the voltage of DC electric field is limited due to the reaction effects of the fluid with electrodes and also heat generation in the vicinity of positive electrode. Using another kind of electrode is a suggestion to prevent the bubble occurrence practically. In addition, a good mixing can be achieved using an AC electric field, noting that the resulting mixing efficiency is less than that of DC electric field. It should be pointed out that, in most cases, the dangers of an AC electric field are high. Also, many chemical reactions in biotechnology and pharmaceutical processes should take place in a very short period of time (O$\sim$0.01 s).

4.5 Effect of the inlet velocity

Figure 16 illustrates the concentration and streamlines profile in the micro-mixer by applying a DC electric field ($V_o = 30$ V) for different inlet velocities ranging from 0.115 to 2.3 mm/s. The figure reveals that the

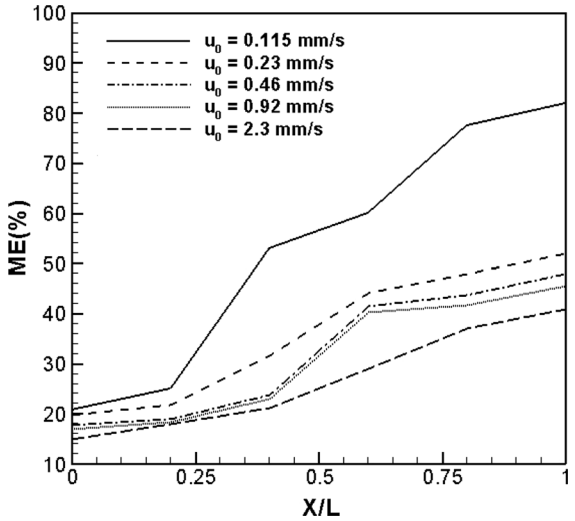

Fig. 17 Mixing efficiency along the micro-mixers for DC electric field with $V_o = 15$ V and different inlet velocities

mixing quality decreases with the inlet velocity. Zhou et al. [13] and Shamloo et al. [14] reported the same conclusion for their proposed micro-mixers. The mixing efficiency is quantitatively plotted in Fig. 17 for different inlet velocities. For the inlet velocities smaller than 0.23 mm/s, the mixing efficiency is very high. For example, it is 82% for the inlet velocity of 0.115. It can be concluded from that the rate of increase in the mixing efficiency is higher for lower inlet velocities.

For small inlet velocities, especially for the velocities smaller than 0.23 mm/s, the molecular diffusion is dominant. By applying the DC electric field, the mixing of two fluids enhances due to the influence of molecular diffusion and electro-osmotic force. As the inlet velocity increases, the remaining time of the fluids in the chamber decreases. In other words, the effect of the molecular diffusion is reduced for high inlet velocities and the electro-osmotic force displaces the fluid layers causes the mixing of the two fluids.

5 Conclusions

The flow field and mixing performance of an electro-osmotic micro-mixer were investigated numerically and experimentally. PDMS was used to fabricate the microchip and gold nanoparticles were used to make the electrodes. Potassium chloride and water were supplied to the micro-mixer from inlet channels. The mixing quality was evaluated when the micro-mixer was under DC and AC electric fields. The results demonstrated that mixing enhancement depends on the vortex generated in the chamber for both electric fields, however DC electric field causes to create stronger vortices in the chamber. It was concluded that mixing efficiency is an increasing function of the applied voltage. The mixing efficiency was 21% and 95.56% for a DC electric field with $V_o = 0$ V and $V_o = 40$ V, respectively. Experimental results revealed that bubbles are generated at high voltages (greater than 25 V for the present geometry). It was also found that the mixing performance decreases with the inlet velocity of the fluids.

References

1. Figeys D, Pinto D (2000) Lab-on-a-chip: a revolution in biological and medical sciences. Anal Chem 72:330A–335A
2. Chin CD, Linder V, Sia SK (2007) Lab-on-a-chip devices for global health: past studies and future opportunities. Lab Chip 7:41–57
3. Lee CY, Chang CL, Wang YN, Fu LM (2011) Micofluidic mixing: a review. Int J Mol Sci 12:3263–3287
4. Chen H, Meiners J-C (2004) Topologic mixing on a microfluidic chip. Appl Phys Lett 84:2193–2195
5. Strook AD, Dertinger SK, Whitesides GM, Ajdari A (2002) Patterning flows using grooved surfaces. Anal Chem 74:5306–5312
6. Strook AD, Dertinger SK, Ajdari A, Mezic I, Stone HA, Whitesides GM (2002) Chaotic mixer for microchannels. Science 295:647–651
7. Cetkin E, Miguel AF (2019) Constructal branched micromixers with enhanced mixing efficiency: slender design, sphere mixing chamber and obstacles. Int J Heat Mass Transf 131:633–644
8. Li T, Chen X (2017) Numerical investigation of 3D novel chaotic micromixers with obstacles. Int J Heat Mass Transf 115:278–282
9. Chen X, Shen J (2017) Numerical analysis of mixing behaviors of two types of E-shaped micromixers. Int J Heat Mass Transf 106:593–600
10. Coleman JT, Sinton D (2005) A sequential injection microfluidic mixing strategy. Microfluidic Nanofluidic 1:319–327
11. Chen H, Zhang Y, Mezic I, Meinhart C, Petzold L (2003) Numerical simulation of an electroosmotic micromixer, Proceeding of IMECE'03, Washington, D.C., pp 15–21
12. Seo H-S, Han B, Kim Y-J (2012) Numerical study on the mixing performance of a ring-type electroosmotic micro-mixer with different obstacle configurations. J Nanofluidic Nanotechnol 12:4523–4530

13. Zhou T, Wang H, Shi L, Liu Z, Joo SW (2018) An enhanced electroosmotic micromixer with an efficient asymmetric lateral structure. Micromachines 7:1–8
14. Shamloo A, Mirzakhanloo M, Dabirzadeh MR (2016) Numerical simulation for efficient mixing of Newtonian and non-Newtonian fluids in an electro-osmotic micro-mixer. Chem Eng Process 107:11–20
15. Shamloo A, Madadelahi M, Abdorahimzadeh S (2017) Three-dimensional numerical simulation of a novel electroosmotic micromixer. Chem Eng Process 119:25–33
16. Meng C, Li H, Tang X, Xu Y (2017) Simulation study on a DC-drive electroosmotic micromixer. Adv Comput Sci Res 74:945–951
17. Cheng Y, Jiang Y, Wang W (2018) Numerical simulation of electro-osmotic mixing under three types of periodic potentials in a T-shaped micro-mixer. Chem Eng Process 127:93–102
18. Usefian A, Bayareh M, Shateri A, Taheri N (2019) Numerical study of electro-osmotic micro-mixing of Newtonian and non-Newtonian fluids. J Braz Soc Mech Sci Eng. https://doi.org/10.1007/s40430-019-1739-2
19. Usefian A, Bayareh M, Ahmadi Nadooshan A (2018) Rapid mixing of Newtonian and non-Newtonian fluids in a three-dimensional micro-mixer using non-uniform magnetic field. J Heat Mass Transf Res. https://doi.org/10.22075/jhmtr.2018.15611.1218
20. Chen X, Wu Z (2019) Design and numerical simulation of a novel microfluidic electroosmotic micromixer with three electrode pairs. J Chem Technol Biotechnol. https://doi.org/10.1002/jctb.5982
21. Sasaki N, Kitamori T, Kim H-B (2010) Experimental and theoretical characterization of an AC electroosmotic micromixer. Anal Sci 26:815–819
22. Wang S-C, Lai Y-W, Ben Y, Chang H-C (2004) Microfluidic mixing by dc and ac nonlinear electrokinetic vortex flows. Ind Eng Chem Res 43:2902–2911
23. Shang X, Huang X, Yang C (2015) Mixing enhancement by the vortex in a microfluidic mixer with actuation. Exp Therm Fluid Sci 67:57–61